Doctoral thesis-2024

Title

Crucial roles of exosomes secreted from ganglioside GD3/GD2-positive glioma cells in enhancement of the malignant phenotypes and signals of GD3/GD2-negative glioma cells

RB21803
Mohammad Abul Hasnat
Department of Biomedical Sciences
Graduate School of Life and Health Sciences
Chubu University

Supervisor
Yoshiyuki Kawamoto
Associate professor
Department of Biomedical Sciences
Chubu University

Mentor
Koichi Furukawa
Professor
Department of Biomedical Sciences
Chubu University

Acknowledgment

At first, I would like to express my earnest appreciation to my supervisor, Dr. Yoshiyuki Kawamoto, Associate Professor, Department of Biomedical Sciences, Chubu University, for his continuous support. and for his patience and knowledge.

Then, I want to express my sincere and heart-felt gratitude to my mentor Prof. Koichi Furukawa, Department of Biomedical Sciences, Chubu University, for his direct supervision and guidance throughout the time of this study as well as for his assistance and unbelievable efforts in writing of this thesis paper and the manuscript of my research work that is accepted by a renowned journal. I also want to express my appreciation to him for his inspiration, motivation, passion, and immense knowledge.

Besides my mentor, I would like to give grateful thanks to Prof. Keiko Furukawa, Department of Biomedical Sciences, Chubu University and Dr. Yuhsuke Ohmi, Assistant Professor, Department of Clinical Engineering, Chubu University, for extending their helping hands in many times during my research periods.

I am cordially thankful to my respected class teachers for their nice and informative presentation in remote classes during Covid-pandemic.

My kind-hearted gratitude is also to Mrs. Mayumi Kojima for her unbelievable administrative assistances and continuous support that made both my student and family life in Japan very convenient.

I am also deeply grateful to my senior and junior lab members and colleagues for their incessant support, great cooperation, and technical assistance.

Finally, I want to give my eternal gratitude to the government of Japan for giving me the world renowned MEXT scholarship which was actual fuel to survive here in Japan.

Contents

List of figures

List of abbreviations

EVs	extracellular vesicles
Exo	exosomes
Sup	supernatant
GD3	Neu5Ac α2,8Neu5Ac α2,3Gal β1,4Glc-ceramide
GD2	GalNAc β1,4(Neu5Ac α2,8Neu5Ac α2,3) Gal β1,4Glc-ceramide
ST8SIA1	alpha-N-acetyl-neuraminide alpha-2,8-sialyltransferase (GD3 synthase)
DMEM	Dulbecco's minimal essential medium
FCS	fetal calf serum
MTT	3-(4,5-dimethylthiazol-2-yl)-2,5-diphenyltetrazolium bromide
RT-CES	real-time cell electronic sensing system
SD	standard deviation
NS	not significant
Tim4	T cell immunoglobulin and mucin domain containing 4
PS	phosphatidylserine
PMSF	phenylmethylsulfonylfluoride
BSA	bovine serum albumin
PBS	phosphate-buffered saline
PBST	Phosphate-buffered saline with Tween 20
IB	immunoblotting
SDS-PAGE	sodium dodecyl-sulfate polyacrylamide gel electrophoresis
mAbs	monoclonal antibodies
FITC	fluorescein isothiocyanate
HRP	horseradish peroxidase
PDGFR	platelet-derived growth factor receptor
MAPK	mitogen-activated protein kinase
FAK	focal adhesion kinase
Erk1	extracellular signal-regulated protein kinases 1
Erk2	extracellular signal-regulated protein kinases 2
kDa	kilodalton
GSLs	glycosphingolipids
EMT	epithelial–mesenchymal transition

Abstract

Neuroectoderm-derived tumors characteristically express gangliosides such as GD3 and GD2. Many studies have reported that gangliosides GD3/GD2 enhance malignant phenotypes of cancers. Recently, we reported that human gliomas expressing GD3/GD2 exhibited enhanced malignant phenotypes. Here, we investigated the function of GD3/GD2 in glioma cells and GD3/GD2-expressing glioma-derived exosomes. As reported previously, transfectant cells of human glioma U251 MG expressing GD3/GD2 showed enhanced cancer phenotypes compared with GD3/GD2-negative controls. When GD3/GD2-negative cells were treated with exosomes secreted from GD3/GD2-positive cells, clearly increased malignant properties such as cell growth, invasion, migration, and cell adhesion were observed. Furthermore, increased phosphorylation of signaling molecules was detected after 5 to15 min of exosome treatment, i.e., higher tyrosine phosphorylation of platelet-derived growth factor receptorβ, focal adhesion kinase, and paxillin was found in treated cells than in controls. Phosphorylation of extracellular signal-regulated kinase-1/2 was also enhanced. Consequently, it is suggested that exosomes secreted from GD3/GD2-positive gliomas play important roles in enhancement of the malignant properties of glioma cells, leading to total aggravation of heterogenous cancer tissues, and also in the regulation of tumor microenvironments.

Graphical abstract

Crucial roles of exosomes secreted from ganglioside GD3/GD2-positive glioma cells in enhancement of the malignant phenotypes and signals of GD3/GD2-negative glioma cells

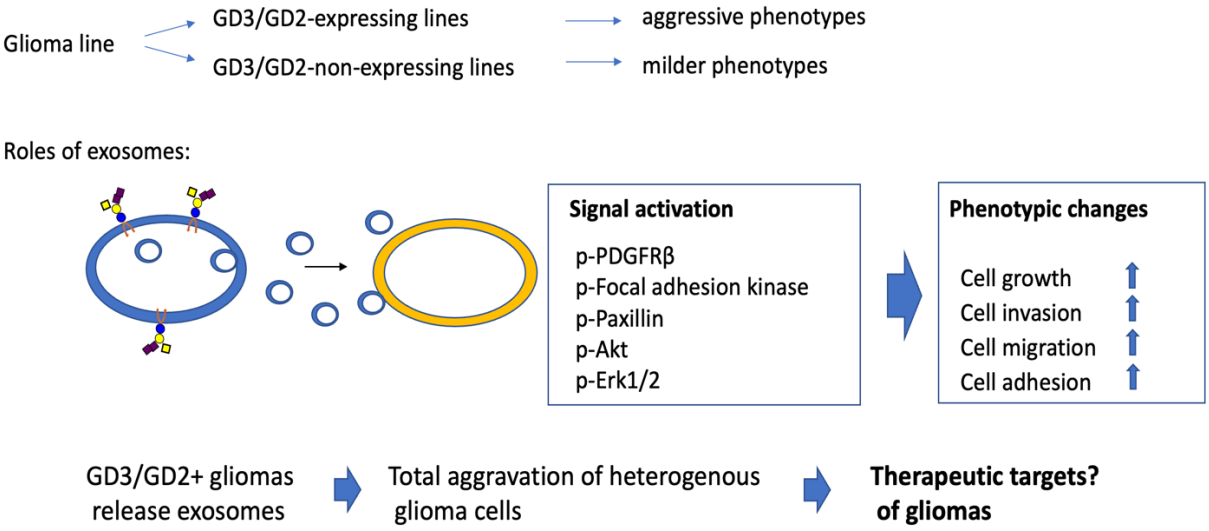

1. Introduction

1.1. Glioma

Gliomas, a type of brain tumor, generally originate from glial cells of the brain or their precursor cells [1], and mostly exhibit a highly invasive activity, and expand outward by infiltrating normal brain tissues [2]. Gliomas constitute around 30% of both brain tumors and central nervous system tumors, representing 80% of malignant brain tumors [3]. Gliomas are classified according to cell type, grade, and location. Based on their growth patterns and infiltrating potential, gliomas are sorted into grades I-IV by the World Health Organization (WHO) [4]. The grade-IV gliomas are the most aggressive type and are also known as glioblastoma (Fig. 1). The glioblastomas often reappear even after a thorough surgical excision; hence they are frequently referred to as recurrent brain cancer [5].

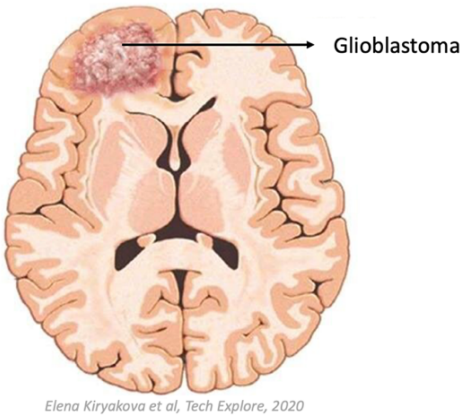

Fig. 1. Human brain and glioblastoma.

1.2. Ganglioside

Gangliosides, sialic acid-containing glycosphingolipids (Fig. 2) are expressed dominantly in nervous tissues and play important roles in the development and functions of central nervous system (CNS). Over 60 gangliosides have been identified, primarily varying in the carbohydrate moiety and number of sialic acids. Complex gangliosides (GM1, GD1a, GD1b and GT1b) are generally expressed during the later stages of brain formation, while simple gangliosides are major structures at the early stage of embryogenesis [6].

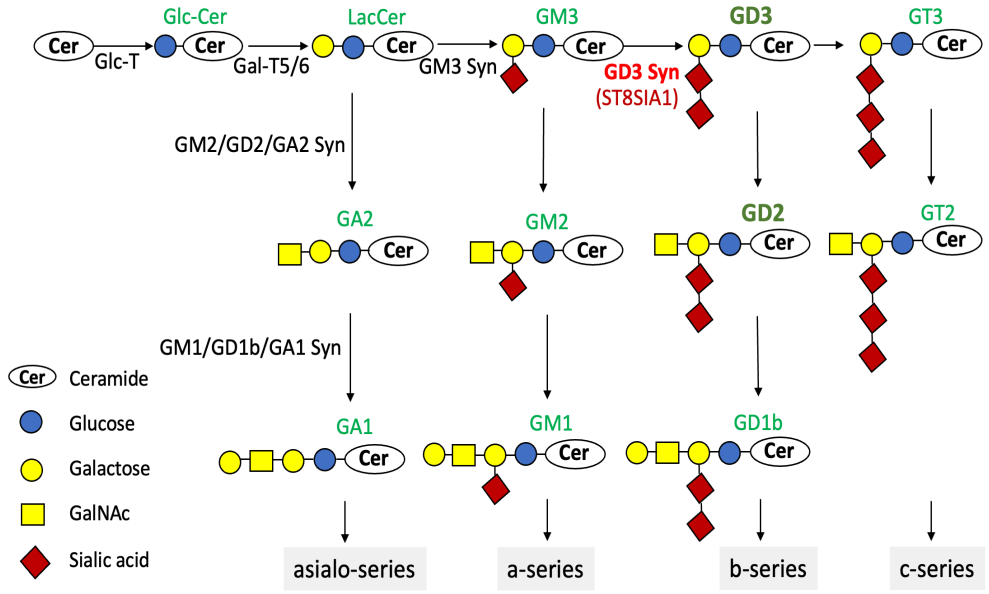

Fig. 2. Biosynthetic pathway of gangliosides.

Some gangliosides like GD3 and GD2 have been reported to be tumor-associated antigens in neuro-ectoderm-derived cancers [7,8], e.g., in melanomas [9] and neuroblastomas [10]. Other human cancers such as small cell lung cancer [11,12] breast cancer [13] and osteosarcoma [14] also characteristically express GD3 and/or GD2. There are some reports of ganglioside expression on gliomas [15,16], but the roles of gangliosides in gliomas are not well-known. Human gliomas also express GD3/GD2, and they are involved in enhancement of the malignant properties [17]. Ganglioside expression in murine gliomas have been analyzed using the RCAS/Gtv-a system, in which expression of GD3/GD2 was shown in induced gliomas, leading to the malignant phenotypes [18]. However, details of the mechanisms leading to these effects have not been sufficiently investigated.

1.3. Extracellular vesicles (EVs)

EVs are lipid bilayer-enclosed particles, naturally released by various normal prokaryotic and eukaryotic cells into the extracellular space [19,20], and also by cancer cells [21]. EVs are classified into two main categories based on their biogenesis: exosomes and ectosomes [22]. Exosomes are small EVs with 40-150 nm in diameter and originate from the endosomal compartment of the cell [22,23,24]. On the other hand, ectosomes with highly variable sizes ranging from 50 to >1000 nm in diameter, form by direct budding of the plasma membrane of cell [22,25,26]. The released exosomes contain many constituents of cells, including DNA, RNA, microRNA [27], lipids, metabolites, and cytosolic and cell-surface proteins [21], and alter the

biological nature of recipient cells [28] (Fig. 3). Several protein markers including CD9, CD63, CD81, Alix, and Tsg101 have been established for the characterization of exosomes [29].

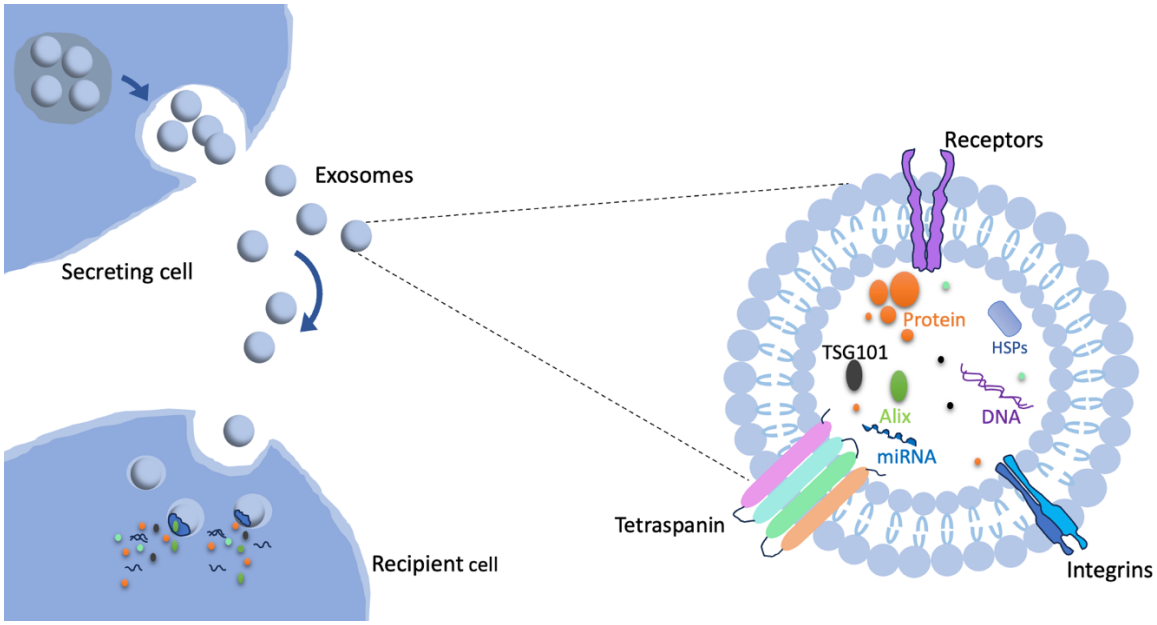

Fig. 3. Exosome functions for cell-to-cell communications.

Exosomes are also released by cultured cells into their growth medium [30]. They are considered to be involved in intercellular communication [31]. There have been interesting studies on exosomes released from cancers, i.e., on regulation of the cancer microenvironment [32,33], and on cancer metastasis [34,35].

1.4. Purposes of the study

Since gliomas are resistant to the current therapy and difficult to control due to their invasive nature, leading to a very poor prognosis [36,37], it is very important to clarify the roles of GD3/GD2-expressing glioma-derived exosomes in the regulation of malignant properties of glioma cells and surrounding normal cells to develop novel strategies for glioma treatment. Findings observed in this study would greatly contribute in the novel therapeutic approaches targeting GD3/GD2-expressing gliomas. The core objectives of this study are to clarify the vital roles of exosomes secreted from the ganglioside GD3/GD2-positive glioma cells in the enhancement of malignant properties and signals of GD3/GD2-negative glioma cells.

2. Materials and methods

2.1. Cell lines and cell culture

The cell lines used in this study were GT16, GT18, GT29, CV2, CV3, and CV5. GD3/GD2-positive cell lines (GT16, GT18, and GT29) were generated by transfecting GD3 synthase cDNA [38] and neo-resistant gene into a human glioma cell line, U-251 MG (from JCRB Cell Bank, Osaka, Japan) using pMIKneo vector (Fig. 4).

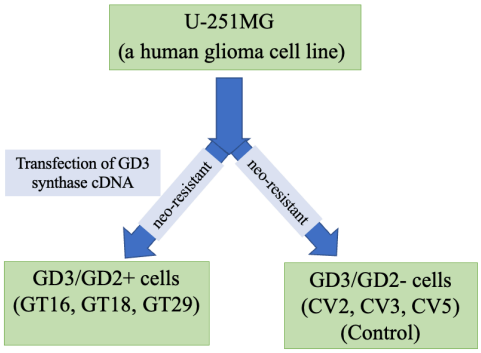

Fig. 4. Generation of GD3/GD2+/- cells by genetic engineering.

The cDNAs of GD3 synthase gene (Fig. 2) were inserted at Xho1 site of pMIKneo vector (Fig. 5). The control cell lines (CV2, CV3, and CV5) were also generated from the U-251 MG cell line by transfecting the neo-resistant gene only.

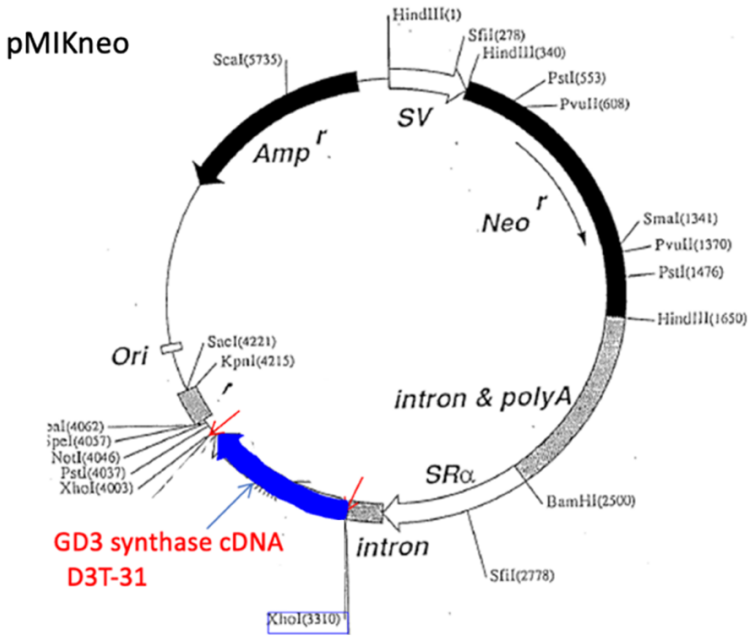

Fig. 5. Introduction of an expression vector of GD3 synthase cDNA.

The cells were cultured in Dulbecco's modified Eagle's medium (DMEM) containing 7.5% fetal calf serum (FCS) and G418 (400 μg/mL) at 37°C in a humidified atmosphere containing 5% CO_2.

2.2. Antibodies and reagents

Anti-GD3 monoclonal antibody (mAb), R24 was provided by L.J. Old at the Memorial Sloan Kettering Cancer Center (New York). Anti-GD2 mAb, 220–51, was generated in our laboratory [39]. The other antibodies and reagents used in this research were obtained from various commercial sources as follows: fluorescein isothiocyanate (FITC)-conjugated goat anti-mouse IgG (H+L) (Cat. No. 55514) from Cappel (Durham, NC, USA), and horseradish peroxidase (HRP)-conjugated anti-mouse IgG antibody (Cat. No. 7076S) and HRP-conjugated anti-rabbit IgG antibody (Cat. No. 7074S) from Cell Signaling Technology (Danvers, MA, USA). Mouse anti-phosphotyrosine antibody, PY20 (Cat. No. sc-508) and mouse Tsg101 (C-2) (Cat. No. sc-7964) were purchased from Santa Cruz Biotechnology (Santa Cruz, CA, USA). Anti-CD9 (Cat. No. 014-27763) and anti-CD63 mAbs (Cat. No. 012-27063) were from Fujifilm Wako (Osaka, Japan). Anti-CD81 mAb (Cat. No. 66866-1-Ig), and anti-Alix polyclonal antibody (12422-1-AP) were from Protein Tech. San Diego, California, USA. Tim4-beads (Cat. No. 297-79701), PS Capture Exosome Flow Cytometry kit (Cat. No. CC050), 2-amino-2 hydroxymethyl-1, 3-propanediol (Cat. No. 201-06273), Giemsa (Cat. No. 079-04391) and BSA (Cat. No. LEH3163) were obtained from Fujifilm Wako (Osaka, Japan). The ImmunoStar LD (Cat. No. 290–69,904) detection kit, G418 (Cat. No. 076-05962), sodium hydrogen carbonate (Cat. No. 191–01,305), sodium dodecyl sulfate (Cat. No. 196–08,675), ammonium peroxodisulfate (Cat. No. 016-20501), and N, N, N1, N1—tetramethyl-ethylenediamine (Cat. No. 205-06313) were also from Wako. Matrigel (Cat. No. 354234) was from BD Bioscience (San Jose, CA, USA), and collagen-1 (Cat. No. CC050) and Tween20 (Cat. No. P2287) were from Sigma-Aldrich. Protease Inhibitor Mixture (Cat. No. 539131) was from Calbio-chem (San Diego, CA, USA), and cell lysis buffer (Cat. No. 9803S) was from Cell Signaling. MTT (3-(4,5-dimethylthiazol-2-yl)-2,5-diphenyltetrazolium bromide) (Cat. No. 349-01824) was from Dojindo Laboratories, Kumamoto, Japan. FCS (REF 04-007-1A) was from B1 Biological Industries (Kibbutz Beit-Haemek, Israel). FastGene BlueStar prestained protein marker (Cat. No. MWP03-8) was from Nippon Genetics Europe GmbH, Duren, Germany. Phenylmethylsulfonylfluoride (PMSF) (Cat. No. 10837091001) was from Roche Diagnostics GmbH, Mannheim, Germany.

2.3. Isolation of exosomes from culture supernatants of glioma cells

EVs were isolated from cultural supernatants of glioma cells (Fig. 6). Confluent cells, 70-80% in 15 cm dishes were washed three times with cold 1xPBS and cultured with DMEM containing 1% ITS premix (Corning™ ITS premix universal culture supplement, Thermofisher Scientific, MA, USA) for 48 h. Culture supernatants were transferred in 50 mL falcon tubes and centrifuged at 4°C and 500×g for 10 min. After centrifuging again at 4°C and 20,000×g for 20 min, the supernatants were filtered using 0.22 µm Sartolab filters (RF-150) (Zartorius, Helsinki, Finland) and transferred into Beckman polypropylene ultracentrifuge tubes (Beckman Coulter, Brea, CA, USA).

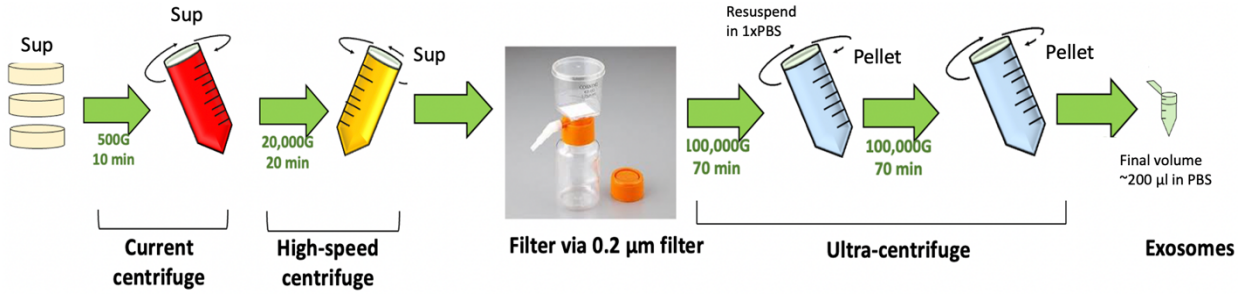

Fig. 6. Exosome isolation and collection.

Then, the samples were centrifuged at 175,000 g and 4°C for 84 min using Beckman SW32Ti rotor (Kent MI, USA). After discarding the supernatants and vortexing, sediments were suspended in cold 1xPBS, and the samples were rotated at 175,000 g and 4°C for 84 min again. After removal of the supernatants, the samples were slightly vortexed, and 200 µL of cold 1xPBS was added. The samples were then used immediately or stored at -80°C after aliquoting. An exosome sample in 1xPBS was used for measuring the protein amount using DC protein assay kit (Bio-Rad, Hercules, CA, USA) or Pierce BCA Protein Assay Kit (Cat. No. 23225, Thermofisher Scientific). To characterize the preparations, we performed immunoblotting (IB) of exosome markers, i. e., tetraspanins (CD9, CD63, CD81), Alix, and Tsg101.

2.4. Flow cytometry

Expression levels of the gangliosides GD3 and GD2 on the cell surface were analyzed by the Accuri™ C6 flow cytometer (BD Biosciences, USA) [40,41]. Briefly, following the trypsinization of cells, the cells ($5x10^5$) were incubated with diluted primary antibodies in 1xPBS for 60 min

on ice. After washing, cells were stained with diluted secondary antibodies, FITC-conjugated goat anti-mouse IgG (H + L) (Cappel), in 1xPBS for 45 min on ice. Then, the relative expression levels were analyzed by a flow cytometer. Control samples were prepared using non-relevant mAbs with the same subclasses as the individual primary antibodies. The CFlow plus™ program was used for the data analysis.

In the case of exosomes, the expression levels of tetraspanins, GD3, and GD2 on exosomes were analyzed by Tim4-beads (Fig. 7).

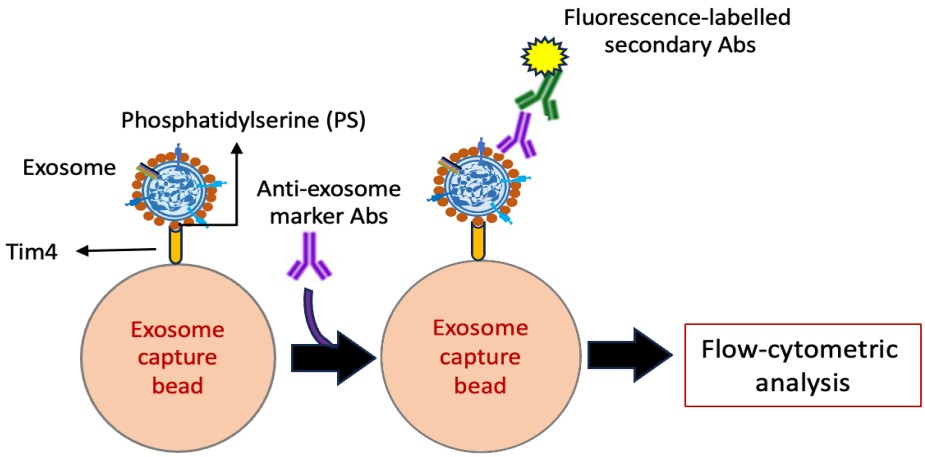

Fig. 7. Tim4-beads flow cytometry.

Exosomes were mixed with PS-capture™ Tim4-beads for 1 h at room temperature (RT) with light vortexing every 10 min. Exosome-bound Tim4-beads were washed twice using a magnetic stand (290-35591, FUJIFILM Wako), and primary antibodies against exosome markers (CD9, CD63, CD81, Alix, and Tsg101), GD3, and GD2 were added and incubated for 1 h on ice. After washing, exosomes bound to Tim4-beads were applied for flow cytometry as explained above.

2.5. MTT assay (cell proliferation assay)

Cells ($3x10^3$) were seeded in each well of 96-well plates with 100 µL of DMEM supplemented with various concentrations of FCS: 0, 0.1, 0.5, 4.0, and 7.5%. To examine the effect of exosomes on cell proliferation, exosomes were added just after the addition of cells [42]. MTT solution (5 mg/mL 1xPBS, 20 µL) was added on days 0, 1, 2, 4, and 5, and incubated for 6 h in a 5% CO_2 incubator at 37°C. After 6 h, 150 µL of acidic 2-propanol (0.4% HCl and 0.1% NP-40 containing 2-propanol) was added to stop the reaction in each well, and it was vigorously

pipetted to destroy cells. About 100 µL of cell lysates were transferred into a new 96-well plate and absorbance was measured at 595-620 nm by an automatic microplate reader (Thermofisher Scientific, Type: 357, Shanghai, China).

2.6. Invasion assay

Cell invasion activity was analyzed with the Boyden-chamber method (Fig. 8) [43]. Cell culture inserts (Transparent PET^{TM} membrane, 24-well format, 8.0-µm pore size, Life Sciences, Durham, NC, USA) were used. For polymerization, Matrigel (a solubilized basement membrane preparation extracted from EHS mouse sarcoma, BD Bioscience, 20 µL) in cold PBS (200 µg/mL) was applied to the upper chamber of the cell culture inserts and incubated for 2 h at room temperature in a current clean bench. After removing PBS, the upper chamber was filled with 200 µL of serum-free DMEM and incubated for 1 h, and the lower chamber was filled with DMEM containing 7.5% FCS. GD3/GD2 (+) and (-) cells (3×10^4) in 200 µL of serum-free DMEM were added in the upper chamber after removal of serum-free medium.

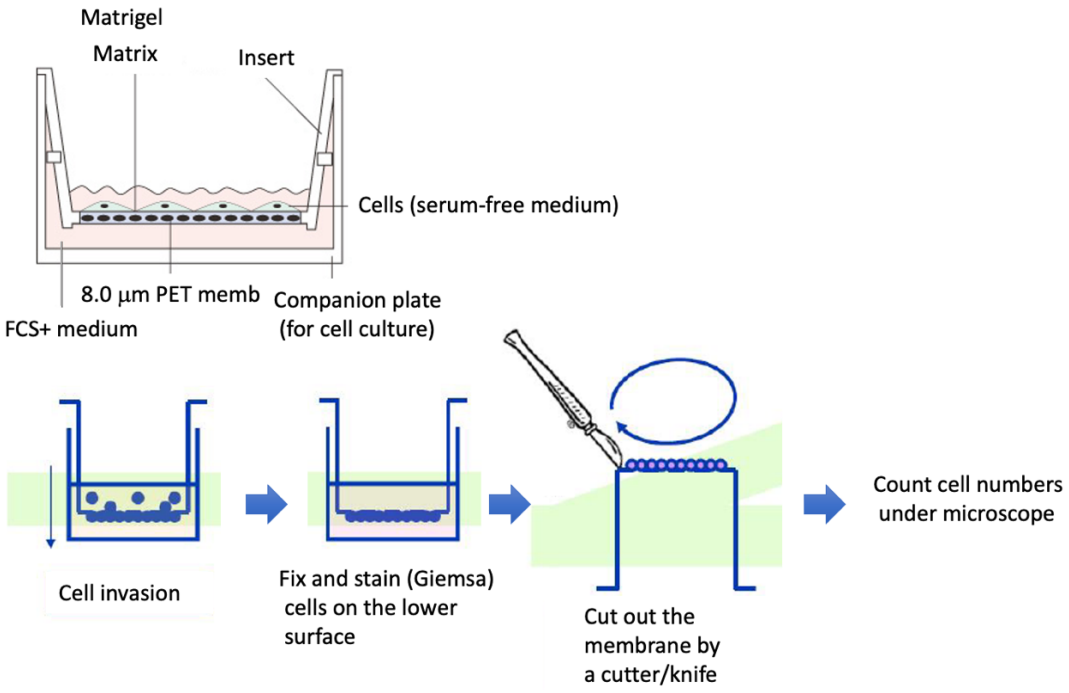

Fig. 8. Measurement of invasion activity by Boyden chamber.

To analyze the effect of exosomes on the invasion activity of cells, exosomes were added after the addition of cells and incubated for 24 h at 37°C in a humidified atmosphere containing 5% CO_2 [44]. After incubation, the numbers of cells that had migrated to the reverse side of the

chamber were counted under a microscope (IX73P1F^{TM}, Olympus, Tokyo, Japan) after being fixed and stained with Giemsa (Wako, Osaka, Japan).

2.7. Migration assay

Two-dimensional migration activity of cells was measured with a wound healing scratch motility assay [45]. The GD3/GD2(+) and GD3/GD2(-) cells ($3x10^5$) were seeded in 6-cm dishes with 7.5% FCS-containing DMEM. After 70-80% confluence, cells were scratched with pipette tips (Pipette Tips RC UNV 250 µL 1000A/1). To observe the effect of exosomes on the migration activity of cells, 250 µL exosomes (4 µg/dish) were added after cell scratching. Individual cell migration was observed under a microscope (IX73P1F^{TM}, Olympus, Tokyo, Japan), and pictures of the scratched regions were taken at different time-points: 0, 4, 8, 12, 18, and 24 h. Then the wound-healing activities were measured and expressed as % to the initial wound lengths.

2.8. Cell adhesion assay

The adhesion activity of cells was measured using the real-time cell electronic sensing system (RT-CES^{TM}) (Fig. 9) (Wako), as describe previously [46].

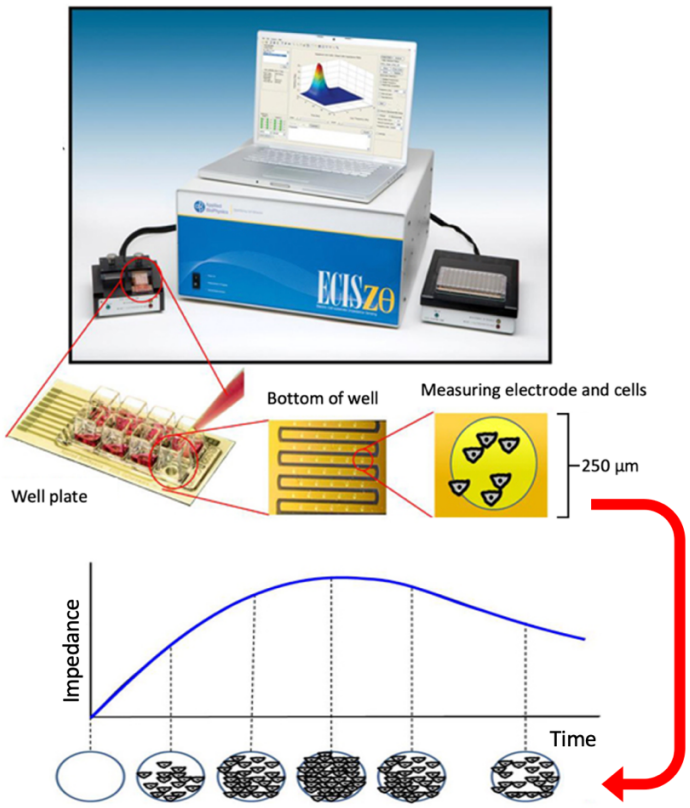

Fig. 9. Real-time cell electronic sensing system (RT-CES)

An E-plate/ microplate with electronic sensor was used to detect the cell adhesion activity. At the bottom of the microplates (E-Plate (16X) (ACEA Biosciences Inc., San Diego, CA, USA), microelectronic cell sensor arrays are integrated. The sensor on the micro-well of the microplate provides information on the increased electrical resistance (cell index), indicating the increase in cell adhesion. E-plates were coated with collagen-1 (CL-1) (5 µg/mL in PBS, 100 µL/well) at RT for 1 h, and blocked by 1% BSA/7.5% FCS in DMEM (100 µL/well) at RT for 1 h. After blocking the micro-wells and removal of BSA solution, cells ($1x10^4$) were seeded in each well of the microplates containing the culture medium. To examine the effect of exosomes on cell adhesion activity, exosomes were added at time 0. The changes in cell adhesion were monitored continuously, and are expressed as the cell index (CI).

2.9. Preparation of cell and exosome lysates

An established method of cell lysate preparation was used [43,47]. Brifly, cultured cells on 6-cm dishes were washed three times with PBS, and then cell lysates were prepared by scraping the cells following the addition of lysis buffer (20 mM Tris-HCl, 1 mM EGTA, 1 mM Na_2EDTA, 150 mM NaCl, 1% Triton X-100, 1 mM β-glycero-phosphate, 2.5 mM sodium pyrophosphate, 1 mM Na_3VO_4, and 1 µg/mL leupeptin) (Cell Signaling), supplemented with 1 mM PMSF and Protease Inhibitor Mixture™ (Calbiochem) to the dishes. The collected lysates were centrifuged at 3000 rpm (Kubota 3740TM, Tokyo, Japan) for 5 min at 4°C to remove insoluble cell debris. After repeated centrifugation, the supernatants were used to measure the protein concentration using the DC protein assay kit (Bio-Rad). In the case of exosomes, the isolated exosomes in PBS were used to prepare exosome lysates. Lysis buffer was added to lyse exosomes at 1:1 ratio on ice for 5 min, and well mixed by pipetting. The protein concentration of the prepared lysates was measured using the DC protein assay kit (Bio-Rad).

2.10. Immunoblotting (IB)

After preparing the lysates, the proteins were separated by SDS–PAGE 10% agarose gels [43,47]. A sample buffer consisting of 125 mM Tris-HCl (pH 6.8), 4% SDS, 20% glycerol, 0.1% bromophenol blue, 4% 2-mercaptoethanol was mixed with lysates at a 1:1 ratio, and boiled for 5 min at 95°C before protein separation. The separated proteins in gels were transferred onto an Immobilon-P membrane (EMD Millipore, Burlington, MA, USA), and blots were blocked for 1 h/overnight with 5% skim milk in PBS with 0.05% Tween-20 (PBST). The reaction

with the primary antibody was performed for 1 h at RT/overnight at 4°C. After washing with PBST, the reaction with the secondary antibody was carried out for 1 h at RT. After washing, bands of proteins were visualized using ImmunoStar™ LD detection kits (Wako), and band images were analyzed with Amersham Imager (Model: 680 software version 2.0, GE Healthcare, Uppsala, Sweden). Anti-β-actin antibodies were used to ensure equal amount of protein loading in each well.

2.11. Statistical analysis

Statistical analyses were done as previously described [42]. Data are presented as the mean ± SD. The data were analyzed by an unpaired Student's two-tailed t-test, and two-way ANOVA with the Tukey post-hoc test to compare mean values. These results were indicated in each individual figure legends. P-values of <0.05 were considered significant. Significance was analyzed using R software (version 3.6.3).

3. Results

3.1. Expression of gangliosides and EV marker proteins on cell surfaces and EVs

GD3/GD2(+) cell lines (GT16, GT18, and GT29) were established by transfecting a human glioma cell line, U-251 MG (GD3/GD2 non-expressing), with GD3 synthase cDNA, and GD3/GD2(-) cell lines (CV2, CV3, and CV5) were vector controls [17]. The surface expression of GD3/GD2 in each group as analyzed by flow cytometry was shown in Fig. 10.

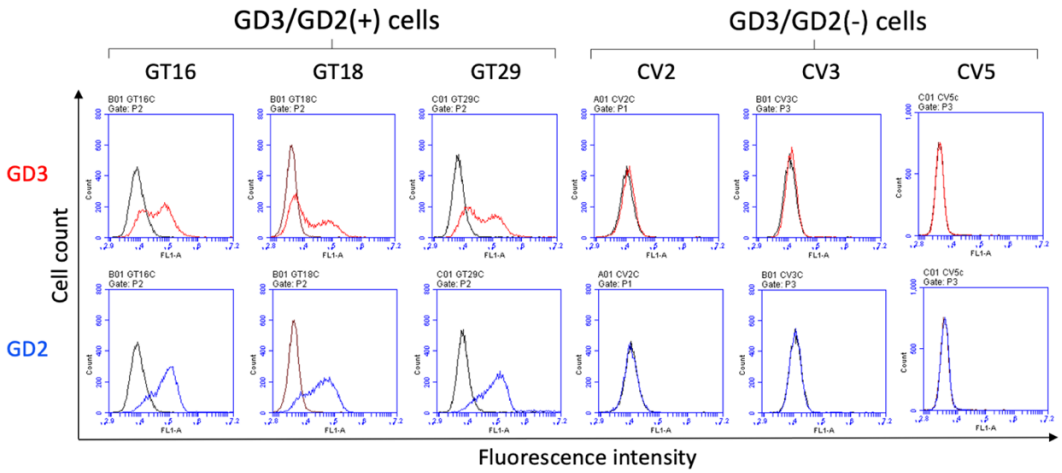

Fig. 10. Cell surface expression of GD3/GD2 on the established GD3/GD2(+) and GD3/GD2(-) clones as analyzed by flow cytometry.
GD3 and GD2 were expressed on the established GD3/GD2(+) clones (left) but not on GD3/GD2(-) clones (right).

The expression of tetraspanins (CD9, CD63, and CD81) known as EV markers was also compared between GT16 (GD3/GD2+) and CV2 (GD3/GD2-) cell lines, showing no clear differences in flow cytometry (Fig. 11A). EVs derived from GT16 and CV2 cells were analyzed with Tim4-beads flow cytometry to investigate expression levels of gangliosides and EV markers. GT16 cell-derived EVs expressed GD3 and GD2, but CV2 cell-derived EVs did not (Fig. 11B). Similar expression of CD81 and CD63 was detected on both types of EVs, while that of CD9 was much higher on EVs derived from GT16 cells (Fig. 11B).

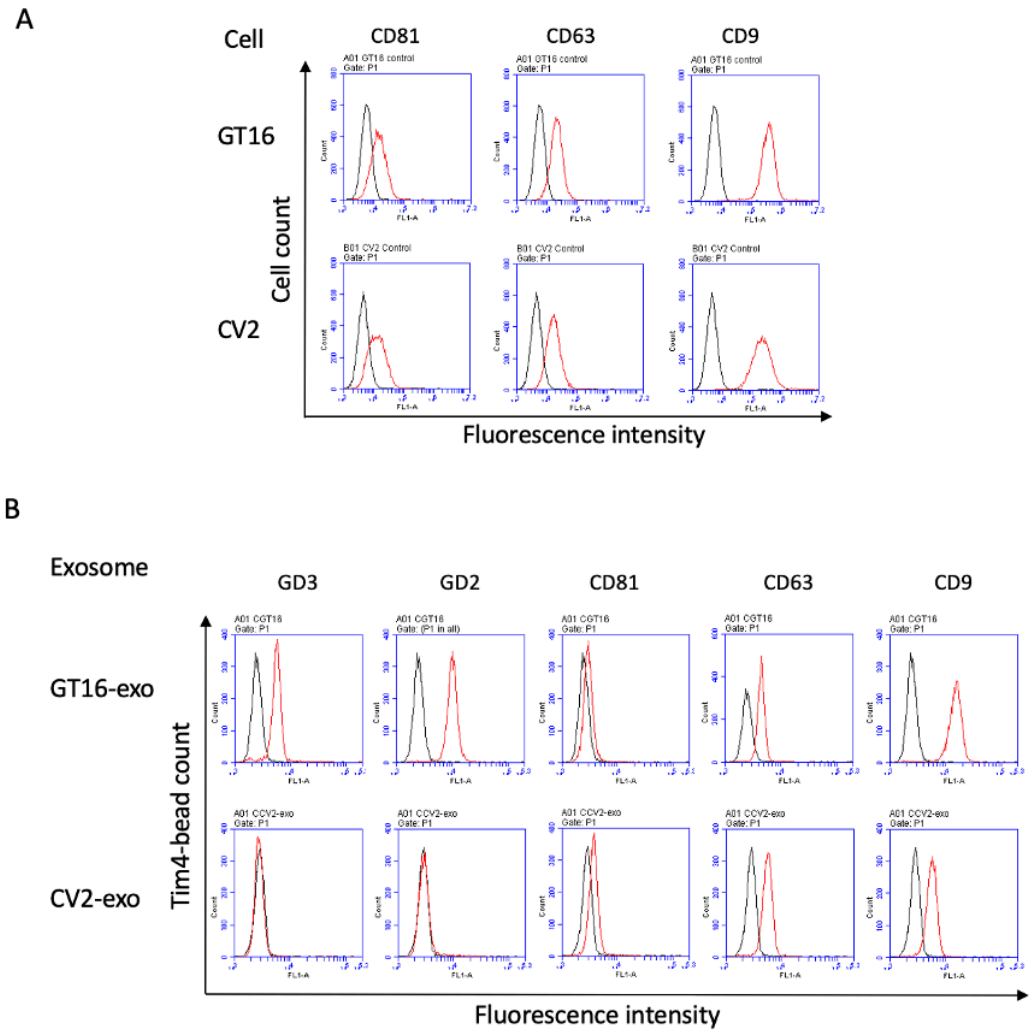

Fig. 11. Expression of EV marker proteins on surface of cells and EVs.
(A) Expression of tetraspanins on GD3/GD2(+) GT16 cells and on GD3/GD2(-) CV2 cells as analyzed by flow cytometry. Anti-CD81, anti-CD63, and anti-CD9 mAbs were used as primary antibodies, and FITC-labeled secondary antibody was employed. **(B)** Expression of tetraspanins and gangliosides on exosomes was analyzed using Tim4-beads flow cytometry as described in A.

3.2. Expression of EV marker proteins in cell lines and EVs as analyzed by IB

IB of lysates from cells and EVs derived from GT16 and CV2 cells was performed using specific mAbs for EV markers. Similar levels of Alix were detected in the lysates from GT16 and CV2 cells, while the GT16 cell lysate contained slightly higher levels of CD9, CD81, and Tsg101 than CV2 cell lysates (Fig. 12A). Higher expression of CD63 was observed in the CV2 cell lysate (Fig. 12B). Lysate from GT16 cell-derived EVs showed higher levels of CD9 than that from CV2 cells (Fig. 12A), while CD81, Alix, CD63, Tsg101, and CD63 showed almost equal bands in EVs from CV2 cells and GT16 cells (Fig. 12A and B).

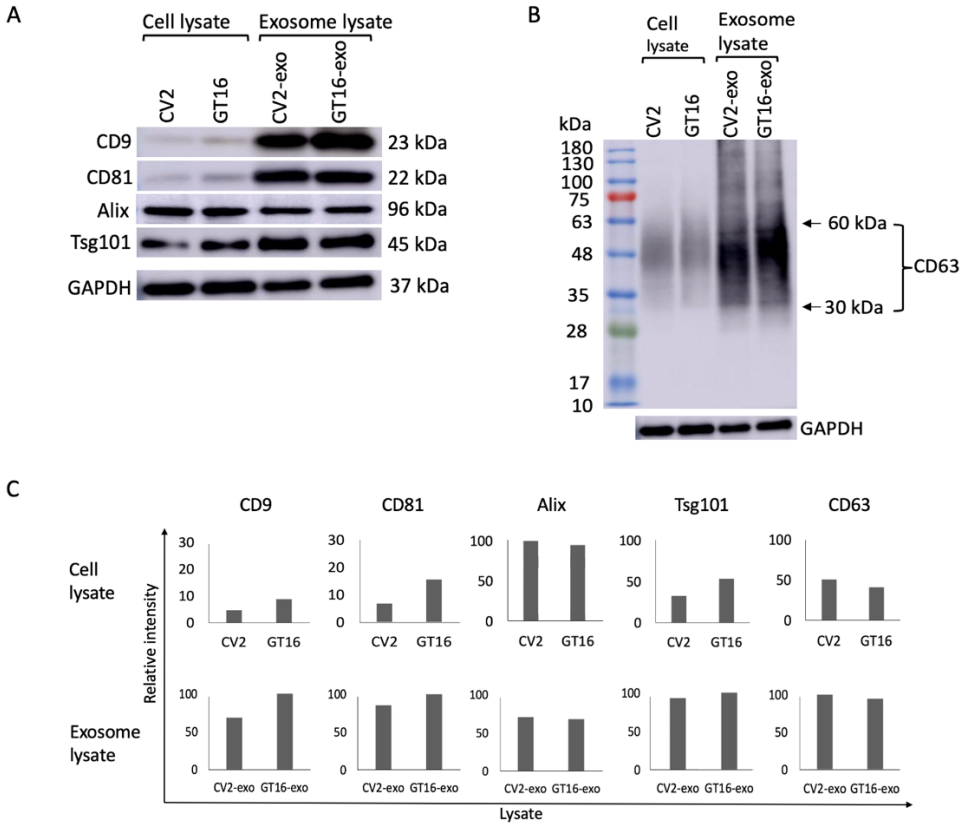

Fig. 12. Expression of EV marker proteins in cells and EVs

(A) IB of cell lysates (CV2 and GT16) and exosome lysates (derived from CV2 cells and GT16 cells) was performed using specific primary antibodies. IB was performed using antibodies reactive with EV markers, e.g., CD9, CD81, Alix, and Tsg101. **(B)** The results of IB of cell lysates and EVs lysates with anti-CD63 mAb. **(C)** Band intensities (CD9, CD81, Alix, Tsg101, and CD63) were measured by Amersham Imager 680 Analysis Software 2.0 and plotted. Representative results from repeated experiments (at least 3 times) are presented.

3.3. Effects of GD3/GD2 and EVs on cell phenotypes

In order to analyze the effects of EVs (derived from GD3/GD2+ GT16 and GD3/GD2- CV2 cells) on the phenotypes of GD3/GD2(-) and (+) glioma cells, the proliferation rate, invasion, migration, and adhesion activities of cell lines were investigated.

3.3.1. Proliferation rate analysis

To investigate the proliferation rate of GD3/GD2-expressing and non-expressing cell groups, the MTT assay was carried out in the presence or absence of EVs. In 7.5% FCS-containing DMEM, almost equivalent cell growth rates of all cell lines were found (Fig. 13A, left). However, a higher growth rate of GT16 cells than CV2 cells was found in 4% FCS-containing DMEM (Fig. 13A, right). Under this condition, CV2 cells showed significantly increased cell growth after treatment with GT16 cell-derived EVs in a dose-dependent manner (Fig. 13B, left). On the

other hand, when EVs released from CV2 cells were added to the culture medium of GT16 cells, the growth rate was reduced (Fig. 13B, right).

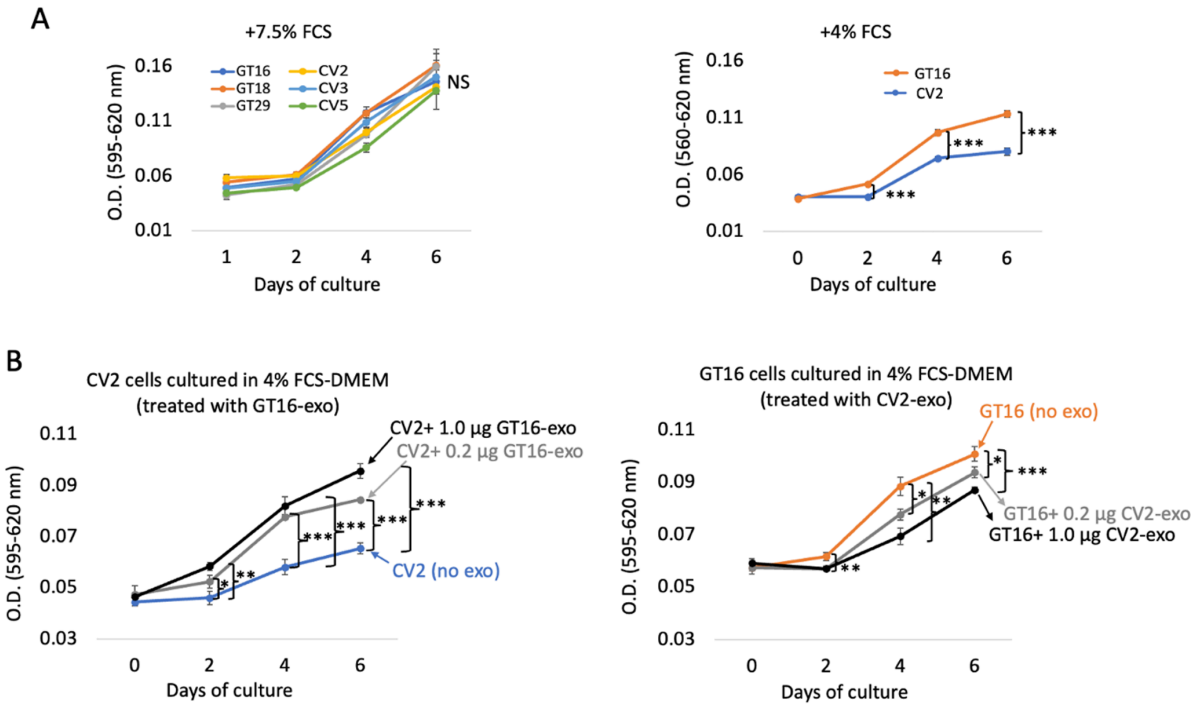

Fig. 13. Cell growth of GD3/GD2(+) and (-) cells and effects of exosomes.
(A) The cell proliferation rate was compared between GD3/GD2(+) cells and GD3/GD2(-) cells in medium containing 4.0 and 7.5% FCS by the MTT assay. The MTT assay was performed by seeding cells in 96-well plates, and by measuring absorbance at 595-620 nm. Relative absorbance was plotted. Three each of sample group cells were examined by two-way ANOVA. GD3/GD2(+) cells exhibited a higher cell growth when cultured under an FCS concentration of 0-4%, but not in 7.5% (*p<0.05, **p<0.01, and ***p<0.001). **(B)** Effects of EVs on growth of GT16 and CV2 cells were analyzed in 4% FCS-DMEM in the presence or absence of EVs. CV2 cells were treated with GT16 cell-derived EVs (0.2 and 1.0 μg), and showed an increased proliferation rate. In contrast, GT16 cells were treated with CV2 cell-derived EVs (0.2 and 1.0 μg), resulting in the suppression of cell growth. Each analysis was performed in triplicate, and the mean ± SD is presented. The data on days 0, 1, 2, 4, 5 and 6 were analyzed by two-way ANOVA with a Tukey post hoc test. *P < 0.05, **P < 0.01, and ***P < 0.001.

3.3.2. Analysis of invasion activity

The cell invasion activity examined by the Boyden-chamber assay revealed that GD3/GD2(+) cells showed significantly higher invasion activity than GD3/GD2(-) cells (Fig. 14A and B). Then, invasion activity of GD3/GD2(-) CV2 cells was analyzed after the addition of EVs released from GD3/GD2(+) cells, showing that the invasion activity gradually increased with the addition of EVs, as shown in Fig. 14C and D. On the other hand, GD3/GD2(-) cell-derived EVs suppressed the invasion activity of GT16 cells (Fig. 14E and F).

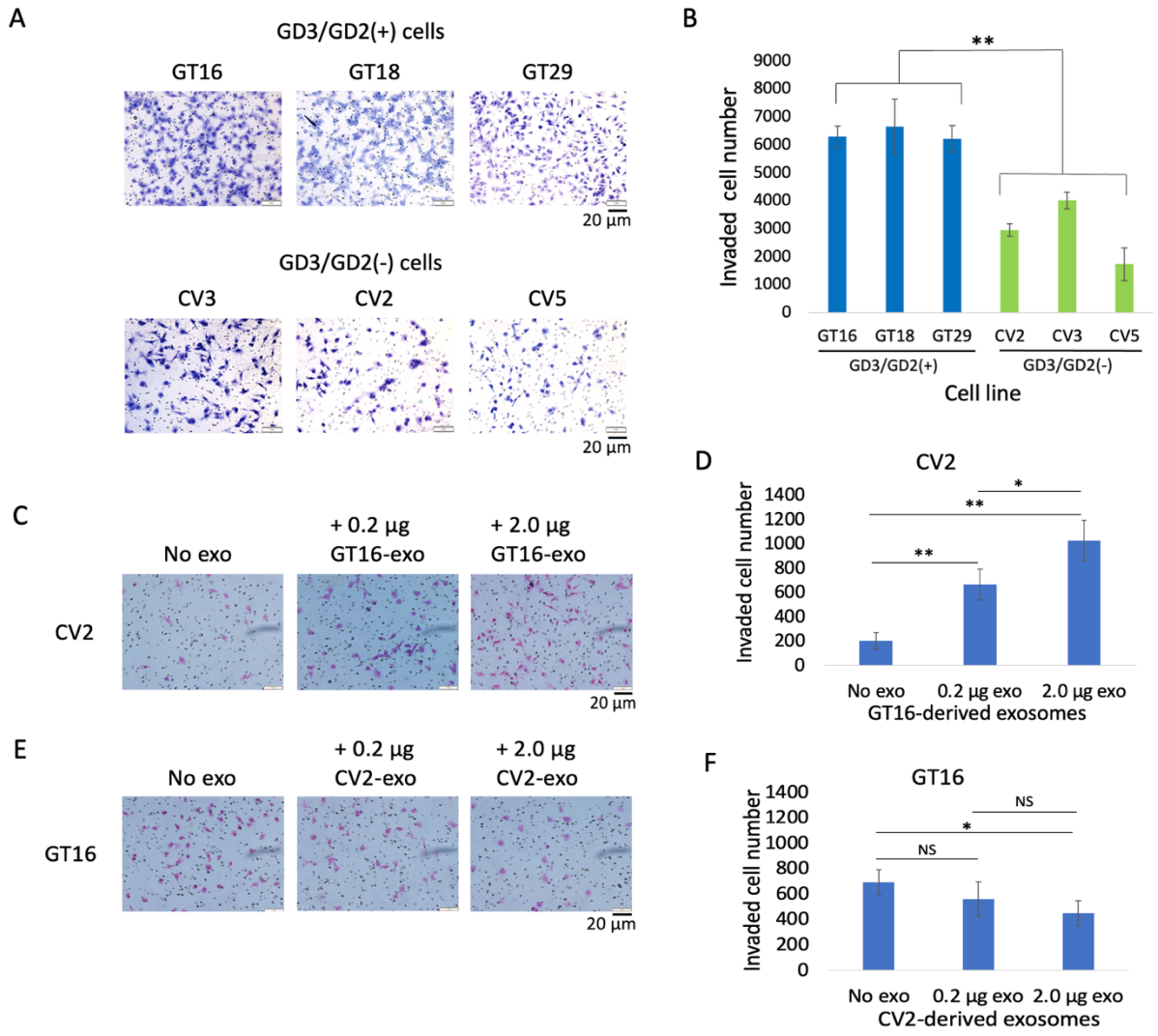

Fig. 14. Invasion activity of GD3/GD2(+) and (-) cells, and effects of EVs.
(A) Microscopic images of invaded cells of both groups, GD3/GD2(+) and (-). Invasion activity was examined by the Boyden-chamber assay. The upper chamber was coated with Matrigel. After 24 hrs of incubation, invaded cells on the reverse side of the membranes were counted under microscope following Giemsa staining. **(B)** The counted cell numbers (A) were plotted where GD3/GD2(+) cells showed significantly higher invasion activity (** $p<0.01$) than GD3/GD2(-) cells. The results are presented as means ± SD, and the data were analyzed with an unpaired Student's two-tailed t test. **(C)** Invasion activity of CV2 cells was analyzed after treatment with GT16 cell-derived EVs (0.2 and 2.0 µg). EVs were added after seeding the cells. **(D)** The invaded cell numbers in (C) were plotted, showing that GT16 cell-derived EVs enhanced the invasion of CV2 in a dose dependent manner. The unpaired Student's two-tailed t test was performed for evaluation of the results C. *$P < 0.05$, **$P < 0.01$. **(E)** The invasion activity of GD3/GD2(+) GT16 cells were analyzed after treatment with CV2 cell-derived EVs (0.2 and 2.0 µg), and counted under microscope. **(F)** The counted cell numbers in (E) were plotted, showing a suppressive effect. The analysis was performed in triplicate, and the mean ± SD is presented. The data were analyzed with an unpaired Student's two-tailed t test. *$P<0.05$; **$P<0.01$; and NS, not significant ($P>0.05$).

3.3.3 Investigation of migration activity

Effects of GD3/GD2 and EVs on 2-D migration of cells were investigated with the wound healing scratch assay. The GD3/GD2(+) cell group showed higher migration activity than the control group (Fig. 15A and B). When CV2 cells were cultured with EVs released from GT16

cells, they showed greater tendency to heal the wound areas than the non-EVs control (Fig. 15C and D). However, no significant effect of CV2 cell-derived EVs on the motility of GT16 cells was observed (Fig. 15C and E).

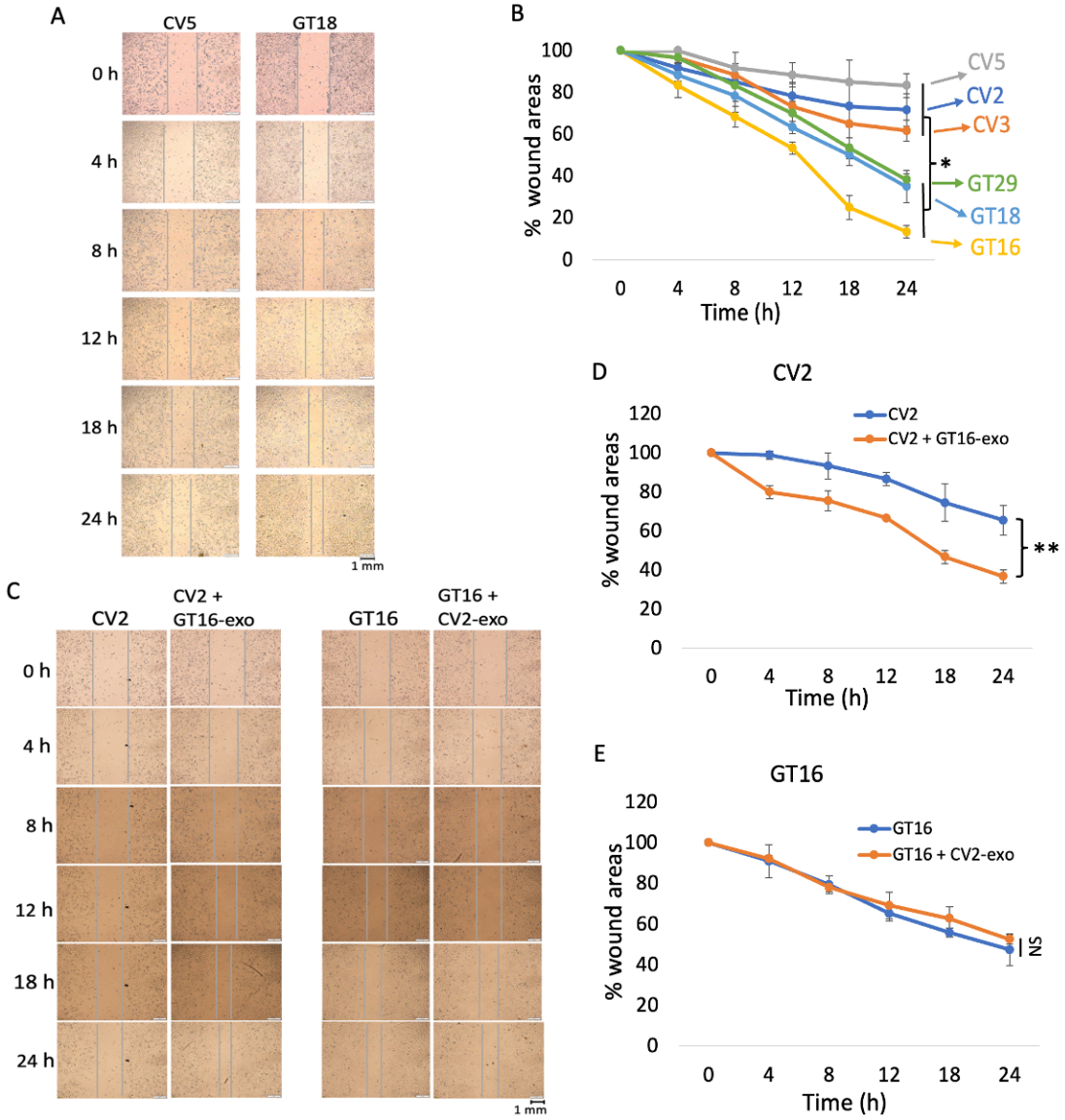

Fig. 15. GD3/GD2(+) cells exhibited higher migration activity, and exosomes derived from them enhanced the migration activity of GD3/GD2(-) cells.
(A) Migration activities of cells were analyzed by the wound healing scratch assay. CV5 and GT18 are representative cell lines from GD3/GD2(-) and GD3/GD2(+) cell groups, respectively. Cells were cultured in 7.5% FCS-containing medium and scratched at around 70-80% confluency. Individual cell migration was observed under microscope and pictures of the scratched regions were taken at the time points indicated. **(B)** Graphical presentation of the migration assay of cells. Wound areas are presented as a percentage of the initial wound size (100%). The mean values ± SD (n=3) were plotted for each time point. GD3/GD2(+) cells showed significantly (*p<0.05) higher motility than the controls. **(C)** Migration activities of CV2 cells and GT16 cells were examined after the addition of EVs (4 μg) derived from GT16 cells and CV2 cells, respectively. Effects of exosomes on wound healing were examined at different time points as indicated. **(D)** The spaces of wound healing were measured and plotted as described in C (left). GD3/GD2(+) cell-derived exosomes significantly (**P < 0.01) increased the

migration activity of GD3/GD2(-) cells. **(E)** The wound healing spaces as described in C (right) were measured at mentioned time points and plotted. No effects of EVs from CV2 cells on invasion of GT16 cells were noted.

3.3.4 Adhesion activity analysis

The adhesion of cells to collagen-I was investigated using real-time cell electronic sensing (RT-CES) system. The GD3/GD2(+) cell group showed a higher tendency to adhere to collagen-I than the GD3/GD2(-) cell group (Fig. 16A). Then, the effect of EVs on cell adhesion was analyzed. When CV2 cells were plated in micro-wells with isolated EVs from GT16 cells, cell adhesion, as presented by the cell index, was increased after one and a half hours depending on the amount of added EVs (Fig. 16B). In contrast, CV2 cell-derived EVs significantly suppressed the adhesion activity of GT16 cells (Fig. 16C) from an early time after addition of EVs.

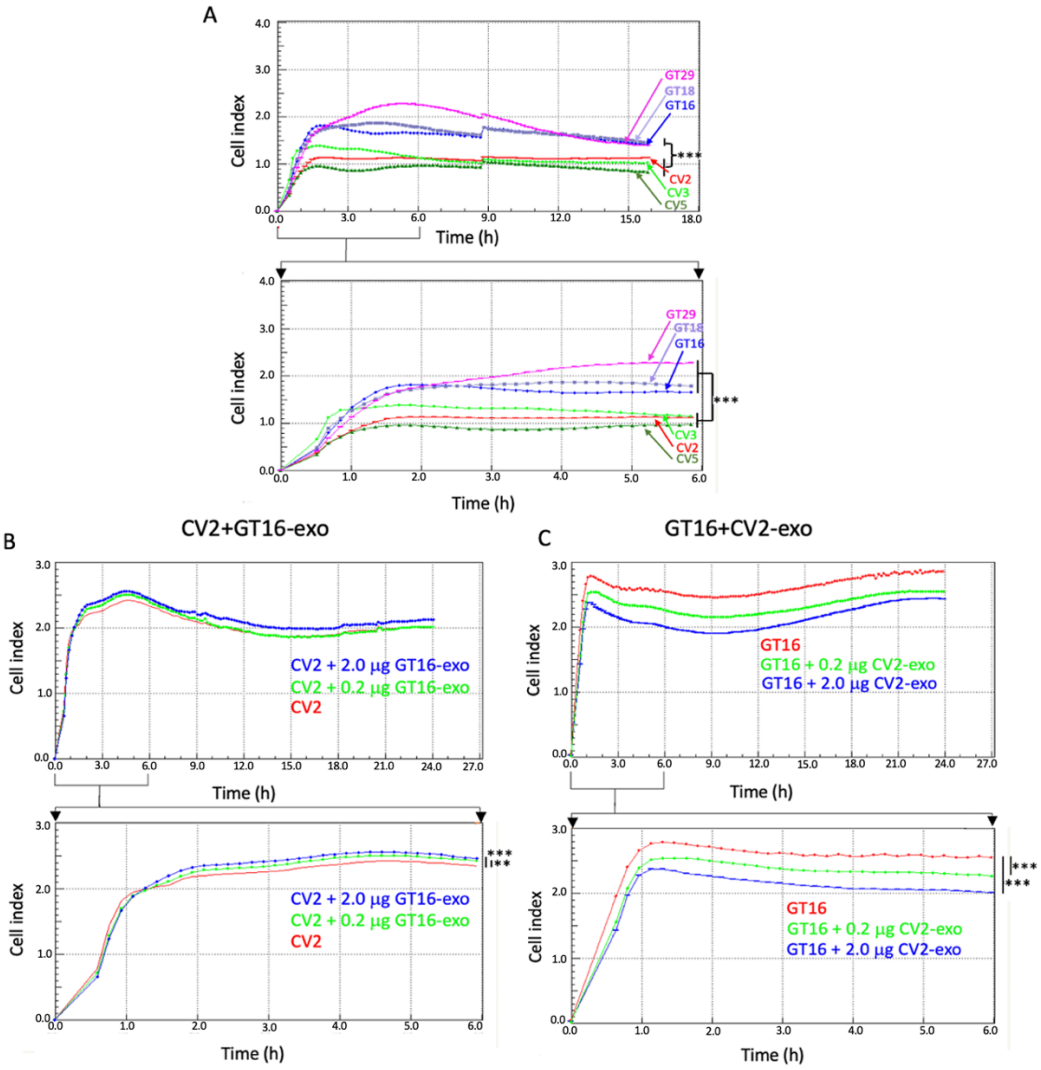

Fig. 16. Effects of GD3/GD2 and exosomes on cell adhesion and the effects of GD3/GD2(+) cell-derived exosomes on cell adhesion.

(A) Adhesion activity of GD3/GD2(+) and (-) cells to collagen-I examined by the real time cell sensing system. Cells ($1x10^4$) were seeded in collagen-I-precoated wells containing 100 µL of culture medium and incubated. The data at 17 h (A, upper) and 6 h (A, lower) of incubation were shown. GD3/GD2 enhanced the adhesion activity of cells. **(B)** Adhesion activity of CV2 cells was investigated after treatment with GT16 cell-derived exosomes. Exosomes (0.2 and 2.0 µg) were added at 0 h, and the changes in cell adhesion are expressed as the cell index. GT16 cell-derived exosomes increased the adhesion activity of CV2 cells. The data until 6 h of incubation (B, lower) were analyzed with an unpaired Student's two-tailed t test. **P < 0.01, and ***P < 0.001. **(C)** GT16 cells were investigated after treatment with CV2 cell-derived exosomes (0.2 and 2.0 µg), resulting in the suppression of adhesion activity in a dose dependent manner. The data until 6 h of incubation (C, lower) were also analyzed with an unpaired Student's two-tailed t test. **P < 0.01, and ***P < 0.001.

3.4. Effects of EVs on the phosphorylation of signaling molecules as analyzed by IB

3.4.1. Effects of GD3/GD2+ GT16 cell-derived EVs on the phosphorylation of signaling molecules of GD3/GD2- CV2 cells during their growth

After being cultured in the FCS-free medium, cells were cultured in 4% FCS- containing DMEM. Then, cell lysates were prepared along the time course indicated in Fig. 17A, and used for IB with anti-phosphotyrosine mAb, PY20. Increased tyrosine-phosphorylated proteins were observed in GT16 cells (Fig. 17B), suggesting that they are FAK, paxillin, and PDGFRβ. The intensity of the three major bands in Fig. 17B were measured and plotted in Fig. 17C. To investigate the effects of EVs derived from GT16 cells on the growth signals in CV2 cells, IB was performed using CV2 cell lysates treated with serum-containing DMEM with or without GT16 cell-derived EVs (Fig. 17D). When cultured in 4% FCS-containing DMEM, a few weak bands were detected by PY20 at 5 min of stimulation (Fig. 17E, left). Strong bands were detected 15 min after the addition of GT16 cell-derived EVs (Fig. 17E, right). The intensity of the three major bands in Fig. 17E was measured and plotted in Fig. 17F.

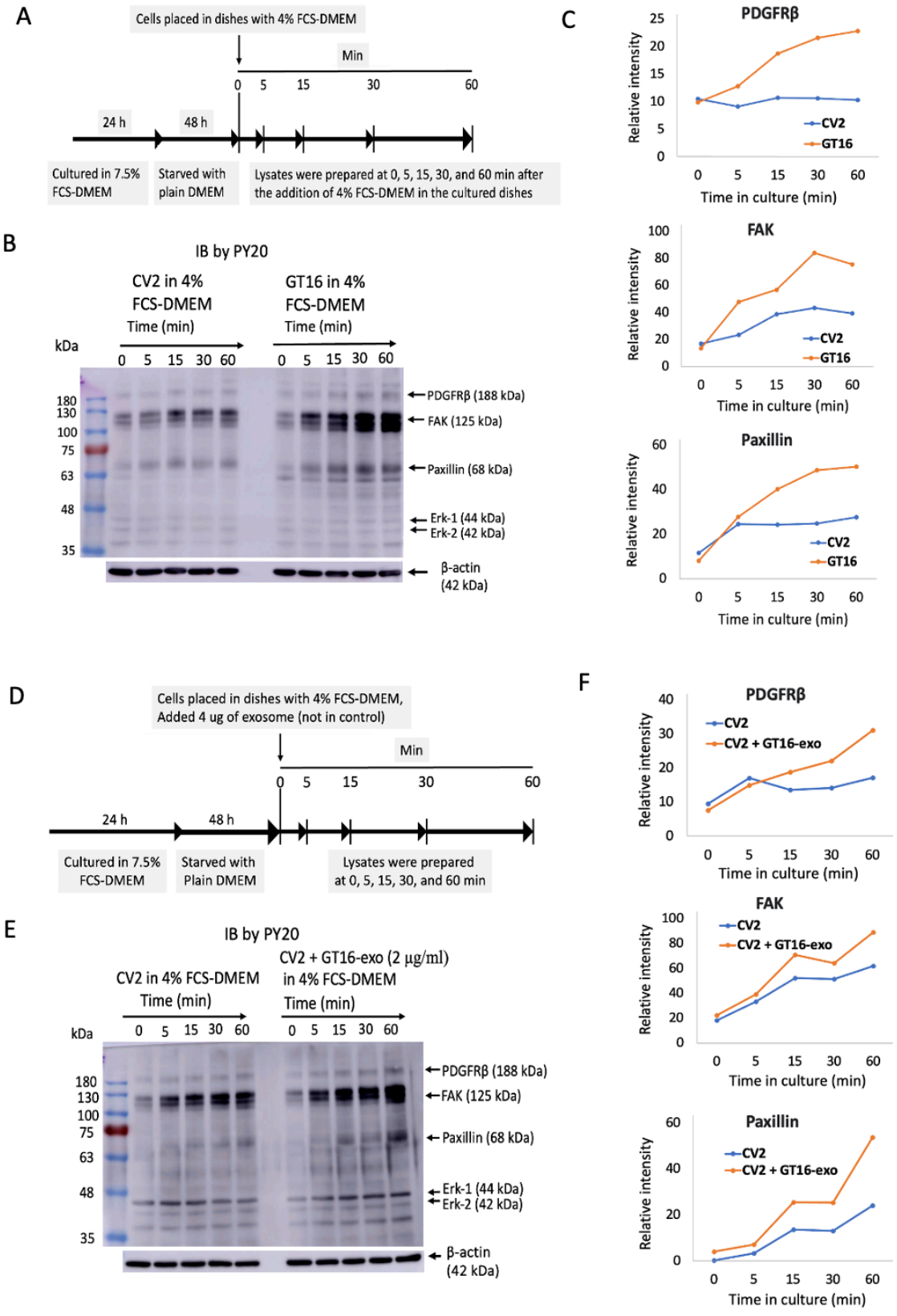

Fig. 17. Effects of exosomes on cell growth signals during cell growth. Tyrosine-phosphorylated protein levels in GD3/GD2(-) cells were increased after treatment with GD3/GD2(+) cell-derived exosomes.
(A) A schema of lysate preparation during cell growth of GD3/GD2(-) cells and GD3/GD2(+) GT16 cells in 4% FCS-DMEM at a various time points of plating after 48 h starvation of serum. **(B)** The prepared lysates (A) were used for IB with PY20. Higher tyrosine phosphorylation was observed in PDGFRβ, FAK, and paxillin of GT16 cells than those in CV2. **(C)** Band intensities at 188, 125, and 68-kDa in B were measured using Amersham Imager 680

software version 2.0, and plotted. **(D)** A schema to prepare lysates during CV2 cell growth in 4% FCS-DMEM in the presence or absence of exosomes derived from GT16 cells at different time points after plating. Cells were prepared as in A. Then cells were cultured in the presence or absence of exosomes (4 μg) derived from GT16 cells in 4% FCS-DMEM, and incubated as indicated. After incubation, the cells were lysed. **(E)** The prepared lysates described in D were subjected to IB with PY20. **(F)** Band intensities in E were measured and plotted in F. Higher tyrosine phosphorylation was observed after ~15 min of EV treatment. Representative results from repeated experiments (at least 3 times) are presented.

3.4.2. Phosphorylation of signaling molecules during cell adhesion

To investigate the effects of GD3/GD2 on intracellular signaling during cell adhesion, we performed IB of CV2 and GT16 cell lysates using PY20 (Fig. 18A and B). After starvation and detaching, cells were placed in collagen-I-precoated dishes with plain DMEM, and cell lysates were prepared as shown in Fig. 18A, and subjected to IB. Phosphotyrosine bands at 5 min were similar in both cell types in Fig. 18B, but after 5 min, bands were stronger in GT16 than CV2 cells. The two major bands in Fig. 18B were scanned and plotted in Fig. 18C. The effects of EVs from GT16 cells on intracellular signaling during adhesion of CV2 cells were examined by preparing CV2 cell lysates in the presence or absence of GT16 cell-derived EVs followed by IB using PY20 (Fig. 18E). Higher phosphorylation in FAK and paxillin was detected in CV2+ GT16-EVs samples after 15 min of treatment (Fig. 18E), and the measured band intensities were plotted in Fig. 18F.

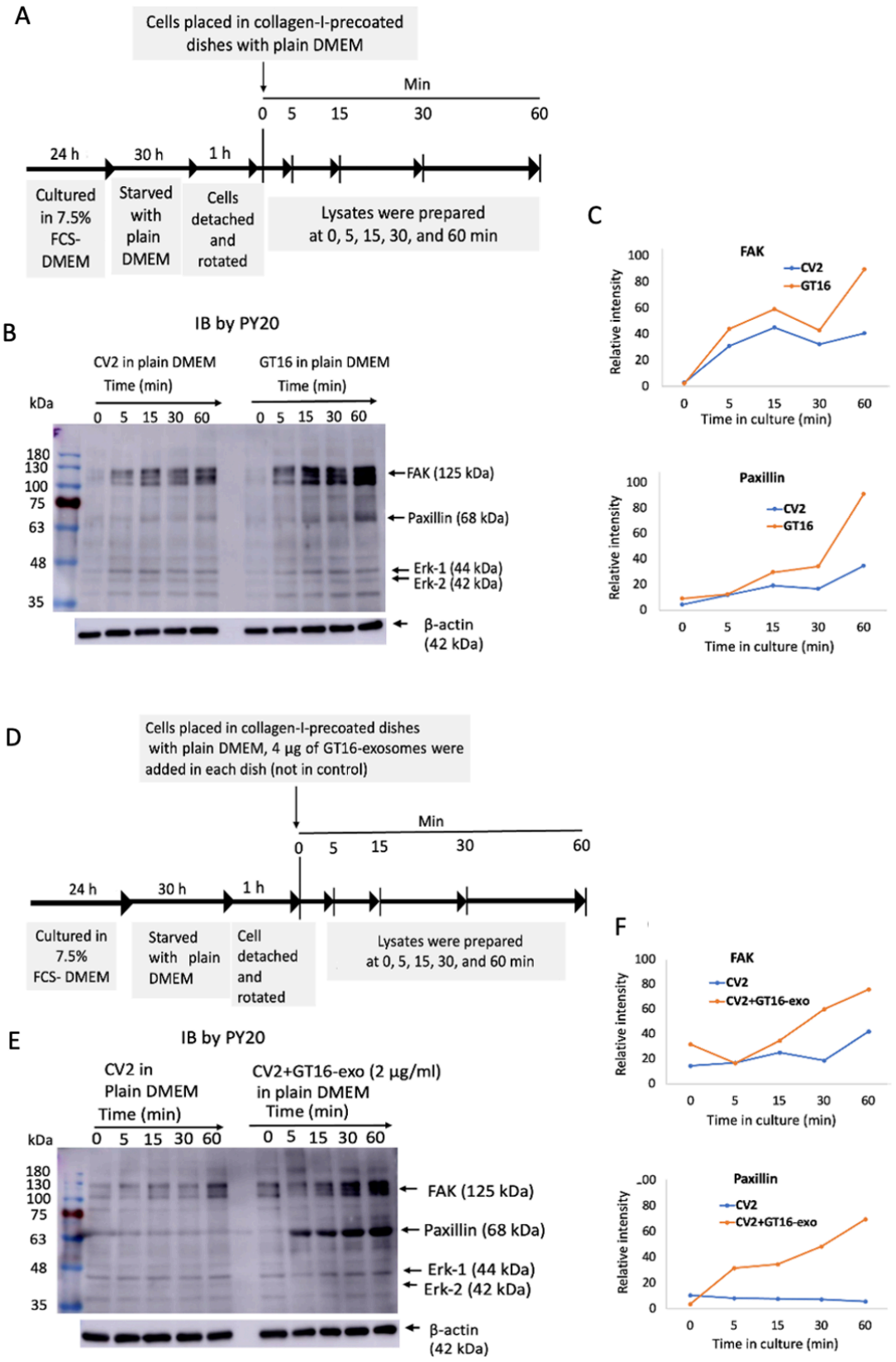

Fig. 18. Effects of exosomes on cell adhesion signals during cell adhesion to collagen-I. Tyrosine-phosphorylated protein levels in GD3/GD2(-) cells were increased after treatment with GD3/GD2(+) cell-derived exosomes. **(A)** A schema for preparing cells to obtain lysates during cell adhesion at various time points. After culture of CV2 cells and GT16 cells in 6-cm dishes with regular medium, cells were starved in plain DMEM for 30 h. After cells were detached, the cell suspension was rotated at 37°C for 1 h. Then, cells were placed in collagen-I-precoated plates in DMEM, and incubated for 0 ~ 60 min at 37°C. After incubation, the cells were lysed. **(B)** The prepared

lysates mentioned in A were used (4 μg/well) for IB using PY20, and images were taken. **(C)** Band intensities in B were measured and plotted. Bands of FAK and paxillin in GT16 cells were higher than CV2 cells after 5 min of incubation. **(D)** A schema of preparing CV2 cells to obtain lysates during their adhesion to collagen-I in the presence or absence of exosomes derived from GT16 cells at several time points. Cells were placed in a collagen-I-precoated plate (6 cm) in plain DMEM, and incubated for 0 ~ 60 min at 37°C in the presence or absence of EVs (4 μg) derived from GT16 cells. After incubation, the cells were lysed. **(E)** The prepared lysates were subjected to SDS-PAGE (4 μg/well). Subsequently, IB was performed with PY20. **(F)** Band intensities in E were measured using Amersham Imager 680 software version 2.0, and plotted. Representative results from repeated experiments (at least 3 times) are presented.

4. Discussion

Functions of cancer-associated glycosphingolipids (GSLs) have been rigorously studied for many years [7], especially after genetic engineering of carbohydrate expression in cultured cells and experimental animals became possible based on the cDNA cloning of glycosyltransferases [48]. Although the roles of a number of cancer-associated GSLs have been reported, those of disialyl gangliosides such as GD3 and GD2 were major subjects in the recent cancer glycobiology research [49]. Our group as well as many others have reported changes in malignant phenotypes and intracellular signals in glyco-remodeled cancer cells, i.e., malignant melanomas[43,46,50], small cell lung cancers [51], osteosarcomas [14], and gliomas [17]. GSLs exert their roles in the microdomains on the cell surface membrane, modulating the structures and functions of membrane molecules [7] and/or modulating intracellular signaling pathways, leading to more malignant phenotypes like increased cell growth, invasion, migration and cell adhesion. Sometimes, enhanced epithelial–mesenchymal transition (EMT) has been demonstrated [52,53].

As for roles of cancer-associated GSLs in exosomes, there have been few reports to date. Recently, we reported functions of GD2 on exosomes in the aggravation of malignant melanomas [42]. While there are many reports on exosomes from gliomas [54], no studies on glycolipids in exosomes in gliomas have been reported. In this study, we analyzed roles of GD3/GD2 in exosomes for the first time, showing that GD3/GD2 in exosomes exert important roles in human glioma cells in their functions that were reported to be effects of cancer-associated gangliosides on the cell surface [17]. Consequently, exosomes released from GD3/GD3-expressing glioma cells enhanced cell growth, invasion, migration and cell invasion as shown in human melanomas [42]. Furthermore, exosomes derived from GD3/GD2-expressing gliomas induced increased phosphorylation levels of the PDGF receptorβ, FAK,

paxillin, and Erk1/2. These results suggest that these signal activations represent the molecular basis for enhanced malignant phenotypes.

Based on the detected signal activation profiles and time-courses, it may be expected how exosomes target recipient cells and modulate their phenotypes. The facts that many signaling molecules underwent phosphorylation after 5 min (PDGFRβ, some FAK sites) or 15 min at the latest (paxillin, some FAK sites) of exosome treatment suggest that these effects are induced through some receptors on the target cell surface, but not by the expression of functional molecules introduced into the recipient cells [55]. The modes of action of exosomes remain to be investigated.

When compared with effects of exosomes derived from GD2-expressing melanoma cells on GD2-negative cells [42], enhancements of cell adhesion was less in glioma system. Furthermore, Tsg101, Flotillin-1 and tetraspanin levels were almost equivalent between GD3/GD2(+) and GD3/GD2(-) glioma cells, while they increased in GD2(+) melanoma-derived exosomes, suggesting that different mechanisms of exosomes are working among individual cancer types as we previously reported in the function analysis of cancer-associated gangliosides [56].

In this study, we analyzed the effects of exosomes derived from GD3/GD2-expressing gliomas on the nature of GD3/GD2-negative gliomas, showing clear functions in phenotypic changes and signal enhancement of target cells. However, cancer tissues generally comprise heterogenous cell populations, and exosomes may play roles in the aggravation of cancer cell features, leading to higher levels of malignant cell groups. Exosomes released from glioma cells may also play important roles in regulation of the tumor microenvironment [57], and cancer metastasis as reported [58]. So, roles of exosomes in regulation of the surrounding normal cell components in cancer tissues are equally important to understand their comprehensive significance and for the construction of novel anti-glioma treatment strategies.

5. References

1. Huse JT, Holland EC, et al. Targeting brain cancer: advances in the molecular pathology of malignant glioma and medulloblastoma. Nat Rev Cancer. 2010;10(5):319-331. doi:10.1038/nrc2818
2. Xie Q, Mittal S, Berens ME, et al. Targeting adaptive glioblastoma: an overview of proliferation and invasion. Neuro Oncol. 2014;16(12):1575-1584. doi:10.1093/neuonc/nou147
3. Goodenberger ML, Jenkins RB, et al. Genetics of adult glioma. Cancer Genet. 2012;205(12):613-621. doi: 10.1016/j.cancergen.2012.10.009
4. Louis DN, Perry A, Reifenberger G, et al. The 2016 World Health Organization Classification of Tumors of the Central Nervous System: a summary. Acta Neuropathol. 2016;131(6):803-820. doi:10.1007/s00401-016-1545-1
5. Pasqualini C, Kozaki T, Bruschi M, et al. Modeling the Interaction between the Microenvironment and Tumor Cells in Brain Tumors. Neuron. 2020;108(6):1025-1044. doi: 10.1016/j.neuron.2020.09.018
6. Schengrund CL, et al. Gangliosides: Glycosphingolipids essential for normal neural development and function. Trends Biochem Sci. 2015;40(7),397-406. https://doi.org/10.1016/j.tibs.2015.03.007
7. Regina TA, Hakomori SI, et al. Functional role of glycosphingolipids and gangliosides in control of cell adhesion, motility, and growth, through glycosynaptic microdomains. Biochim Biophys Acta. 2008;1780(3):421-433. doi:10.1016/j.bbagen.2007.10.008
8. Yeh SC, Wang PY, Lou YW, et al. Glycolipid GD3 and GD3 synthase are key drivers for glioblastoma stem cells and tumorigenicity. Proc Natl Acad Sci U S A. 2016;113(20):5592-5597. doi:10.1073/pnas.1604721113
9. Lloyd KO, et al. Humoral immune responses to tumor-associated carbohydrate antigens. Semin Cancer Biol. 1991;2(6):421-431.
10. Schulz G, Cheresh DA, Varki NM, et al. Detection of ganglioside GD2 in tumor tissues and sera of neuroblastoma patients. Cancer Res. 1984;44(12 Pt 1):5914-5920.

11. Yoshida S, Fukumoto S, Furukawa K, et al. Ganglioside G(D2) in small cell lung cancer cell lines: enhancement of cell proliferation and mediation of apoptosis. Cancer Res. 2001;61(10):4244-4252.
12. Cheresh DA, Rosenberg J, Mujoo K, et al. Biosynthesis and expression of the disialoganglioside GD2, a relevant target antigen on small cell lung carcinoma for monoclonal antibody-mediated cytolysis. Cancer Res. 1986;46(10):5112-5118.
13. Cazet A, Bobowski M, Rombouts Y, et al. The ganglioside G(D2) induces the constitutive activation of c-Met in MDA-MB-231 breast cancer cells expressing the G(D3) synthase. Glycobiology. 2012;22(6):806-816. doi:10.1093/glycob/cws049
14. Shibuya, Hidenobu, et al. Enhancement of malignant properties of human osteosarcoma cells with disialyl gangliosides GD2/GD3. Cancer Sci. 2012;103,9:1656-64. doi:10.1111/j.1349-7006.2012.02344.x
15. Nakamura O, Iwamori M, Matsutani M, et al. Ganglioside GD3 shedding by human gliomas. Acta Neurochir (Wien). 1991;109(1-2):34-36. doi:10.1007/BF01405694
16. Wikstrand CJ, Fredman P, Svennerholm L, et al. Detection of glioma-associated gangliosides GM2, GD2, GD3, 3'-isoLM1 3',6'-isoLD1 in central nervous system tumors in vitro and in vivo using epitope-defined monoclonal antibodies. Prog Brain Res. 1994;101:213-223. doi:10.1016/s0079-6123(08)61951-2
17. Iwasawa T, Zhang P, Ohkawa Y, et al. Enhancement of malignant properties of human glioma cells by ganglioside GD3/GD2. Int J Oncol. 2018;52(4):1255-1266. doi:10.3892/ijo.2018.4266
18. Ohkawa Y, Zhang P, Furukawa K, et al. Lack of GD3 synthase (St8sia1) attenuates malignant properties of gliomas in genetically engineered mouse model. Cancer Sci. 2021;112, (9):3756-3768. doi:10.1111/cas.15032
19. Zaborowski MP, Balaj L, Breakefield XO, et al. Extracellular Vesicles: Composition, Biological Relevance, and Methods of Study. Bioscience. 2015;65(8):783-797. doi:10.1093/biosci/biv084
20. Yáñez-Mó M, Siljander PR, Andreu Z, et al. Biological properties of extracellular vesicles and their physiological functions. J Extracell Vesicles. 2015; 4:27066. doi:10.3402/jev. v4.27066

21. Dai J, Su Y, Zhong S, et al. Exosomes: key players in cancer and potential therapeutic strategy. Signal Transduct Target Ther. 2020;5(1):145. doi:10.1038/s41392-020-00261-0
22. Buzas EI. The roles of extracellular vesicles in the immune system. Nat Rev Immunol. 2023;23, 236–250. https://doi.org/10.1038/s41577-022-00763-8
23. Witwer KW, Théry C, et al. Extracellular vesicles or exosomes? On primacy, precision, and popularity influencing a choice of nomenclature. J Extracell Vesicles. 2019;8(1):1648167. doi:10.1080/20013078.2019.1648167
24. Kim H, Kim EH, Kwak G, et al. Exosomes: Cell-Derived Nanoplatforms for the Delivery of Cancer Therapeutics. Int J Mol Sci. 2020;22(1):14. doi:10.3390/ijms22010014
25. Li M, Liao L, Tian W, et al. Extracellular Vesicles Derived From Apoptotic Cells: An Essential Link Between Death and Regeneration. Front Cell Dev Biol. 2020;8:573511. doi:10.3389/fcell.2020.573511
26. Wang, Y. et al. Apoptotic cell-derived micro/nanosized extracellular vesicles in tissue regeneration. Nanotechnol Rev. 2022;11, 957–972.
27. Thakur BK, Zhang H, Becker A, et al. Double-stranded DNA in exosomes: a novel biomarker in cancer detection. Cell Res. 2014;24(6):766-769. doi:10.1038/cr.2014.44
28. Valadi H, Ekström K, Bossios A, et al. Exosome-mediated transfer of mRNAs and microRNAs is a novel mechanism of genetic exchange between cells. Nat Cell Biol. 2007;9(6):654-659. doi:10.1038/ncb1596
29. Eguchi T, Sogawa C, Okusha Y, et al. Organoids with cancer stem cell-like properties secrete exosomes and HSP90 in a 3D nanoenvironment. PLoS One. 2018;13(2):e0191109. doi: 10.1371/journal.pone.0191109
30. Spaull R, McPherson B, Gialeli A, et al. Exosomes populate the cerebrospinal fluid of preterm infants with post-haemorrhagic hydrocephalus. Int J Dev Neurosci. 2019;73:59-65. doi:10.1016/j.ijdevneu.2019.01.004
31. Meldolesi J. Exosomes and Ectosomes in Intercellular Communication. Curr Biol. 2018;28(8):R435-R444. doi:10.1016/j.cub.2018.01.059
32. Jin Y, Xing J, Xu K, et al. Exosomes in the tumor microenvironment: Promoting cancer progression. Front Immunol. 2022;13:1025218. doi:10.3389/fimmu.2022.1025218

33. da Costa VR, Araldi RP, Vigerelli H, et al. Exosomes in the Tumor Microenvironment: From Biology to Clinical Applications. Cells. 2021;10(10):2617. doi:10.3390/cells10102617
34. Hoshino A, Costa-Silva B, Shen TL, et al. Tumour exosome integrins determine organotropic metastasis. Nature. 2015;527(7578):329-335. doi:10.1038/nature15756
35. Tian W, Liu S, Li B, et al. Potential Role of Exosomes in Cancer Metastasis. Biomed Res Int. 2019;2019:4649705. doi:10.1155/2019/4649705
36. Seker-Polat F, Pinarbasi DN, Solaroglu I, et al. Tumor Cell Infiltration into the Brain in Glioblastoma: From Mechanisms to Clinical Perspectives. Cancers (Basel). 2022;14(2):443. doi:10.3390/cancers14020443
37. Verdugo E, Puerto I, Medina MÁ, et al. An update on the molecular biology of glioblastoma, with clinical implications and progress in its treatment. Cancer Commun (Lond). 2022;42(11):1083-1111. doi:10.1002/cac2.12361
38. Haraguchi M, Yamashiro S, Yamamoto A, et al. Isolation of GD3 synthase gene by expression cloning of GM3 alpha-2,8-sialyltransferase cDNA using anti-GD2 monoclonal antibody. Proc Natl Acad Sci U S A. 1994;91(22):10455-10459. doi:10.1073/pnas.91.22.10455
39. Zhao J, Furukawa K, Fukumoto S, et al. Attenuation of interleukin 2 signal in the spleen cells of complex ganglioside-lacking mice. J Biol Chem. 1999;274(20):13744-13747. doi:10.1074/jbc.274.20.13744
40. Bhuiyan R H, Kondo R, Furukawa K, et al. Expression analysis of 0-series gangliosides in human cancer cell lines with monoclonal antibodies generated using knockout mice of ganglioside synthase genes. Glycobiology. 2016;26;984-998. doi:10.1093/glycob/cww049.
41. Yesmin F, Bhuiyan RH, Furukawa K, et al. Aminoglycosides are efficient reagents to induce readthrough of premature termination codon in mutant B4GALNT1 genes foumd in families of hereditary spastic paraplegia. J Biochem. 2020; 168:103-112. doi: 10.1093/jb/mvaa041.
42. Yesmin F, Furukawa K, Kambe M, et al. Extracellular vesicles released from ganglioside GD2-expressing melanoma cells enhance the malignant properties of GD2-negative melanomas. Sci Rep. 2023;13(1):4987. doi:10.1038/s41598-023-31216-4

43. Yesmin F, Bhuiyan RH, Ohmi Y, et al. Ganglioside GD2 Enhances the Malignant Phenotypes of Melanoma Cells by Cooperating with Integrins. Int J Mol Sci. 2021;23(1):423. doi:10.3390/ijms23010423
44. Ohkawa Y, Momota H, Kato A, et al. Ganglioside GD3 Enhances Invasiveness of Gliomas by Forming a Complex with Platelet-derived Growth Factor Receptor α and Yes Kinase. J Biol Chem. 2015;290(26):16043-16058. doi:10.1074/jbc.M114.635755
45. Dong Y, Ikeda K, Furukawa K, et al. GM1/GD1b/GA1 synthase expression results in the reduced cancer phenotypes with modulation of composition and raft-localization of gangliosides in a melanoma cell line. Cancer Sci. 2010;101,2039-2047. doi:10.1111/j.1349-7006.2010.01613.x.
46. Ohmi Y, Kambe M, Ohkawa Y, et al. Differential roles of gangliosides in malignant properties of melanomas [published correction appears in PLoS One. 2019 3;14(9):e0222220]. PLoS One. 2018;13(11):e0206881. doi:10.1371/journal.pone.0206881
47. Bhuiyan RH, Ohmi Y, Ohkawa Y, et al. Loss of Enzyme Activity in Mutated B4GALNT1 Gene Products in Patients with Hereditary Spastic Paraplegia Results in Relatively Mild Neurological Disorders: Similarity with Phenotypes of B4galnt1 Knockout Mice. Neuroscience. 2019;397:94-106. DOI: 10.1016/j.neuroscience.2018.11.034.
48. Nagata Y, Yamashiro S, Furukawa K, et al. Expression cloning of beta 1,4 N-acetylgalactosaminyltransferase cDNAs that determine the expression of GM2 and GD2 gangliosides [published correction appears in J Biol Chem. 1994;4;269(9):7045]. J Biol Chem. 1992;267(17):12082-12089.
49. Furukawa K, Ohmi Y, Hamamura K, et al. Signaling domains of cancer-associated glycolipids. Glycoconj J. 2022;39(2):145-155. doi:10.1007/s10719-022-10051-1
50. Hamamura K, Furukawa K, Hayashi T, et al. Ganglioside GD3 promotes cell growth and invasion through p130Cas and paxillin in malignant melanoma cells. Proc Natl Acad Sci U S A. 2005;102(31):11041-11046. doi:10.1073/pnas.0503658102
51. Aixinjueluo W, Furukawa K, Zhang Q, et al. Mechanisms for the apoptosis of small cell lung cancer cells induced by anti-GD2 monoclonal antibodies: roles of anoikis. J Biol Chem. 2005;280(33):29828-29836. doi:10.1074/jbc.M414041200
52. Ohkawa Y, Miyazaki S, Hamamura K, et al. Ganglioside GD3 enhances adhesion signals and augments malignant properties of melanoma cells by recruiting integrins to

glycolipid-enriched microdomains. J Biol Chem. 2010;285(35):27213-27223. doi:10.1074/jbc.M109.087791

53. Nazha B, Inal C, Owonikoko TK et al. Disialoganglioside GD2 Expression in Solid Tumors and Role as a Target for Cancer Therapy. Front Oncol. 2020;10:1000. doi:10.3389/fonc.2020.01000
54. Russo MN, Whaley LA, Marissa N, et al. Extracellular vesicles in the glioblastoma microenvironment: A diagnostic and therapeutic perspective. Mol Aspects Med. 2023;91:101167. doi:10.1016/j.mam.2022.101167
55. Xu W, Yang Z, Lu N, et al. From pathogenesis to clinical application: insights into exosomes as transfer vectors in cancer. J Exp Clin Cancer Res. 2016;35(1):156. doi:10.1186/s13046-016-0429-5
56. Furukawa K, Hamamura K, Ohkawa Y, et al. Disialyl gangliosides enhance tumor phenotypes with differential modalities. Glycoconj J. 2012;29(8-9):579-584. doi:10.1007/s10719-012-9423-0
57. Godlewski J, Krichevsky AM, Johnson MD, et al. Belonging to a network--microRNAs, extracellular vesicles, and the glioblastoma microenvironment. Neuro Oncol. 2015;17(5):652-662. doi:10.1093/neuonc/nou292
58. Naghibi AF, Daneshdoust D, Taha SR, et al. Role of cancer stem cell-derived extracellular vesicles in cancer progression and metastasis. Pathol Res Pract. 2023;247:154558. doi:10.1016/j.prp.2023.154558